



HAL
open science

Antimicrobial peptides: mechanism of action and lipid-mediated synergistic interactions within membranes

Dennis Juhl, Elise Glattard, Christopher Aisenbrey, Burkhard Bechinger

► To cite this version:

Dennis Juhl, Elise Glattard, Christopher Aisenbrey, Burkhard Bechinger. Antimicrobial peptides: mechanism of action and lipid-mediated synergistic interactions within membranes. *Faraday Discussions*, 2021, 232, pp.419-434. 10.1039/D0FD00041H . hal-03600929

HAL Id: hal-03600929

<https://hal.science/hal-03600929>

Submitted on 14 Mar 2022

HAL is a multi-disciplinary open access archive for the deposit and dissemination of scientific research documents, whether they are published or not. The documents may come from teaching and research institutions in France or abroad, or from public or private research centers.

L'archive ouverte pluridisciplinaire **HAL**, est destinée au dépôt et à la diffusion de documents scientifiques de niveau recherche, publiés ou non, émanant des établissements d'enseignement et de recherche français ou étrangers, des laboratoires publics ou privés.

PAPER

Antimicrobial peptides: mechanism of action and lipid-mediated synergistic interactions within membranes

Dennis W. Juhl,^a Elise Glattard,^a Christopher Aisenbrey^{*a}
and Burkhard Bechinger^{*ab}

Received 20th April 2020, Accepted 8th September 2020

DOI: 10.1039/d0fd00041h

Biophysical and structural studies of peptide–lipid interactions, peptide topology and dynamics have changed our view of how antimicrobial peptides insert and interact with membranes. Clearly, both peptides and lipids are highly dynamic, and change and mutually adapt their conformation, membrane penetration and detailed morphology on a local and a global level. As a consequence, peptides and lipids can form a wide variety of supramolecular assemblies in which the more hydrophobic sequences preferentially, but not exclusively, adopt transmembrane alignments and have the potential to form oligomeric structures similar to those suggested by the transmembrane helical bundle model. In contrast, charged amphipathic sequences tend to stay intercalated at the membrane interface. Although the membranes are soft and can adapt, at increasing peptide density they cause pronounced disruptions of the phospholipid fatty acyl packing. At even higher local or global concentrations the peptides cause transient membrane openings, rupture and ultimately lysis. Interestingly, mixtures of peptides such as magainin 2 and PGLa, which are stored and secreted naturally as a cocktail, exhibit considerably enhanced antimicrobial activities when investigated together in antimicrobial assays and also in pore forming experiments applied to biophysical model systems. Our most recent investigations reveal that these peptides do not form stable complexes but act by specific lipid-mediated interactions and the nanoscale properties of phospholipid bilayers.

Introduction

Antimicrobial peptides (AMPs) provide a first line of defense against a multitude of pathogenic microorganisms and can be released rapidly when infections occur.^{1,2} They are part of the innate immunity of a wide variety of species from the plant and animal kingdoms, including humans.³ The corresponding databases list thousands of sequences and many are continuously added.^{4,5} Understanding

^aUniversité de Strasbourg/CNRS, UMR7177, Institut de Chimie, 4, rue Blaise Pascal, 67070 Strasbourg, France

^bInstitut Universitaire de France, France

1 their mechanism of action allows one to design molecules with favorable prop-
2 erties that mirror the essential characteristics of the template compounds. They
3 have also been shown to modulate the immune response of the host organisms.⁶
4 Although peptides have a short half-life in natural environments they can be
5 developed into therapeutics by modification of their composition, by nano-
6 structure formulations that protect them from proteolysis until they reach their
7 target or by fixation to surfaces.⁷⁻⁹

8 In this paper we focus on linear cationic antimicrobial peptides such as
9 magainins which were first discovered in frogs.² These antimicrobial peptides are
10 membrane active and they act by interfering with the barrier function of bacterial
11 lipid bilayers.¹⁰ Because it is more difficult for pathogens to adjust the physico-
12 chemical properties of their cell membranes compared to adjusting the
13 sequence of proteinaceous receptors, the development of multi-resistance is less
14 likely.^{2,11} This, in an era where multi-resistance is a major problem for human
15 health, bears great promise for the development of new lines of antibiotics.

16 **Structural and mechanistic studies of membrane-associated antimicrobial** 17 **peptides**

18 Membrane-associated peptides exhibit large conformational and topological
19 freedom. Thus, biophysical investigations reveal that hydrophobic sequences
20 such as alamethicin preferentially, but not exclusively, adopt transmembrane
21 alignments and form pores made of transmembrane helical bundles.¹² In
22 contrast, linear cationic peptides such as magainins, cecropins or LL37 prefer-
23 entially adopt alignments parallel to the membrane interface and work by
24 different mechanisms that could only be established after decades of research
25 and analysis.¹³ Indeed, guidelines for the design of new compounds can be
26 established from the models that arose from the biophysical and structural
27 studies of cationic amphipathic antimicrobial peptides.¹⁴ As a consequence,
28 a number of antimicrobial small molecule mimetics,^{15,16} pseudopeptides^{17,18} and
29 polymers¹⁹ have been introduced.

30 Once the potential of linear cationic amphipathic sequences as antimicrobials
31 was described, considerable research efforts were dedicated to understanding in
32 detail their mechanisms of action and the underlying structural prerequisites.^{2,20}
33 Upon contact with membranes, linear cationic peptides adopt amphipathic folds,
34 specifically disrupt the integrity of bacterial and fungal membranes,² and/or enter
35 into the cell interior¹⁰ where they can interact with and flocculate anionic
36 macromolecules.¹⁸

37 Whereas magainins adopt random coil structures in aqueous buffer, they
38 exhibit helical conformations in membrane environments. Membrane associa-
39 tion is driven by electrostatic interactions and is reversible. The helices of mag-
40 ainin and other linear cationic antimicrobial peptides are predominantly oriented
41 parallel to the membrane surface.¹⁴ Whereas this surface orientation of magainin
42 2 has been observed under all conditions investigated,^{21,22} PGLa has a more
43 dynamic character. Indeed, in fully saturated membranes PGLa can adopt a broad
44 range of tilt angles, a feature which has also been discussed for mixtures with
45 magainin 2 (*cf.* below). However, when interacting with phospholipid bilayers
46 carrying unsaturated groups, like magainin 2, the PGLa orientation is stable and
47 close to perfectly parallel to the bilayer surface.²²⁻²⁴ In contrast, the much more
48

1 hydrophobic alamethicin preferentially adopts transmembrane helical arrange-
ments, although depending on the conditions orientations along the membrane
surface have also been observed.^{25,26}

5 An amphipathic peptide helix that resides in the bilayer interface at an
alignment parallel to the membrane surface uses more space at the level of the
head group and glycerol regions when compared to the hydrophobic interior.¹⁴
This topology thereby causes substantial disordering at the level of the hydro-
phobic region concomitant with membrane thinning.^{27–29} The bilayer disruption
10 has been estimated to extend over a radius of 50 Å.^{30,31} Molecular dynamics (MD)
simulations provide a view of possible magainin membrane arrangements, where
pores form through stochastic rearrangements of peptides and lipids rather than
well-defined channel structures. In some simulations side chains reach the
opposite bilayer leaflet of a thinned membrane, thus water filled channels
15 appear.^{32,33}

From the ensemble of biophysical data a number of models have emerged
including the formation of toroidal pores made of lipid and peptide,^{34,35} the
presence of a peptide ‘carpet’ covering the bilayer surface and ultimately leading
to membrane disruption,³⁶ or the formation of pores through randomly
20 arranged micelle-like aggregates within the membrane.³⁷ With these ideas in
mind a common model has been proposed where in the presence of external
stimuli such as AMPs, ‘Soft Membranes Adapt and Respond, also Transiently’
(SMART).¹³ Within the SMART model, lipid membranes initially adapt to the
disruptive properties of the peptides, but undergo macroscopic phase transi-
25 tions transiently or permanently, locally or globally when the peptide concen-
tration increases.¹³

Because the lipid physico-chemical properties play an important role in the
SMART model, suggestions where peptide-induced changes in the line tension
form the underlying mechanisms for antimicrobial activity involve related lines of
30 ideas.^{38,39} The membrane physico-chemical properties have also been suggested
to be essential for the selectivity of cationic linear peptides for bacterial over
eukaryotic cells.⁴⁰ Positively charged peptides show an orders-of-magnitude
stronger interaction with membranes carrying a negative surface charge
(bacteria) than with neutral ones (eukaryotes).^{41,42} Furthermore, lipid-mediated
35 mesophase-like arrangements along the membrane surface have been demon-
strated to depend on anionic lipids.⁴³ Finally, the membrane association of
multicationic antimicrobial peptides has also been shown to strongly affect
a number of peripheral membrane proteins.⁴⁴

Mechanistic investigations on the synergistic interactions of antimicrobial peptides

45 Magainin 2 and PGLa are part of a naturally occurring cocktail of peptides in the
skin of *Xenopus laevis* frogs. They have been investigated individually but when
added as a mixture they exhibit a much increased antimicrobial activity when
compared to the individual peptides.⁴⁵ The synergistic activity of the magainin 2–
PGLa mixture is also shown when calcein release from phospholipid liposomes is
studied.^{46–48} The enhanced activity of the peptide mixture was proposed to be due
50 to a combination of fast pore formation by PGLa and increased pore stability due
to magainin 2.⁴⁷

1 NMR structural investigations also indicate that in the synergistic mixture
both bilayer-associated PGLa and magainin are helical and adopt an alignment
parallel to the surface of membranes when these carry unsaturated groups,^{23,49,50}
including supported bilayers made from *E. coli* lipid extracts.⁵¹

5 Cross-linking experiments testing membrane-associated PGLa and magainin 2
each carrying a GGC extension indicate the preferential formation of parallel
dimers.⁵² Of note, fluorescence quenching experiments reveal more densely
packed mesophase arrangements of both peptides in the synergistic mixture.^{14,51}
A reduction in bilayer repeat distance due to the presence of the peptides has also
10 been measured by diffraction methods.^{33,53}

A number of studies are suggestive of small favorable interactions of PGLa and
magainin 2 when both are membrane-associated,^{47,54,55} but these experiments do
not reveal if such interactions are due to direct contacts between the peptides,
long-range electrostatics or driven by the lipid matrix.^{28,56} Notably, synergism has
15 been shown to strongly depend on the lipid head group composition, suggesting
important involvement of the lipids.^{48,51} Furthermore, mutagenesis experiments
point out a role of the F16W, E19Q and carboxy-terminal sites of magainin 2.^{47,57}
Within PGLa, changing residues G7, G11, and L18 or the positively charged K15
and K19 sites has an effect on the synergistic enhancement.⁵⁷

20 Models for the synergistic behaviour between PGLa and magainin 2 have been
proposed based on activity assays and low-resolution structural methods without
being conclusive.^{47,51,57} However, high-resolution investigations of the structure,
topology, dynamics and interactions between peptides and between peptides and
lipids that could clarify how they interact in liquid crystalline membranes are
25 missing.

Solid-state NMR spectroscopy is probably the only method to provide struc-
tural and dynamic information at atomistic resolution. To this end peptides
which are uniformly labelled with stable NMR isotopes are needed.⁵⁸ These can be
30 obtained by bacterial overexpression using a previously described fusion tag
where the antimicrobial peptides are neutralized in tight inclusion bodies within
the bacterial cells.⁵⁹ However, the expression in bacteria prevents carboxy-
terminal amidation which normally occurs for PGLa. Moreover, in the system
established in our laboratory, cleavage from the fusion protein by formic acid
35 introduces an amino-terminal proline to the existing sequences.⁵⁹ Here, using
synthesized peptides with modified termini, we investigated how such changes
affect the antimicrobial activity, helix propensity and synergistic activities of the
peptides. We then investigated how the activities correlate with some of the
40 proposed models, where interactions of the termini have been suggested to be of
key importance. Alternative concepts will be presented which shall be discussed
during the Faraday Discussion meeting.

45 Results

To determine the effects of the altered termini, we produced the following seven
peptides by solid-phase synthesis and tested them for antimicrobial and syner-
gistic activities: PGLa, pPGLa, pPGLc, magainin 2a, magainin 2c, pmagainin 2a
50 and pmagainin 2c, where p indicates an additional N-terminal proline, a indicates
an amide and c indicates a free acid at the C-terminus.

Both PGLa and magainin 2 are known to adopt helical structures in membrane-mimetic and lipid bilayer environments.^{60,61} The structural influence of the termini was determined by liquid-state NMR with the peptides dissolved in either aqueous Tris buffer (pH 7.4) or trifluoroethanol (TFE)/buffer (1 : 3 v/v). Assignments were performed based on two-dimensional ^1H - ^1H TOCSY and ^1H - ^1H NOESY spectra while natural abundance ^1H - ^{13}C HSQC spectra were included to obtain the carbon chemical shifts for secondary structure calculations using the neighbour corrected Structural Propensity Calculator (ncSPC).⁶² In good agreement with previous reports,^{63,64} both PGLa and magainin 2a adopted random coil conformations in aqueous buffer (Fig. 1B and 2B). Surprisingly, slight β -sheet tendencies for extended segments of their sequences were observed

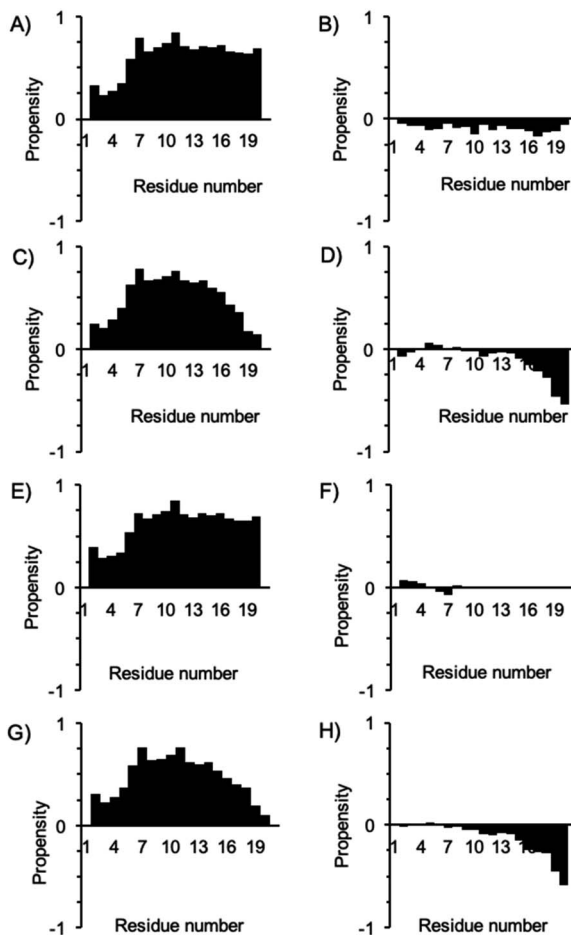


Fig. 1 Helix propensity of PGLa and effects of terminal modifications. Secondary structure propensities determined using assigned chemical shifts and the ncSPC online tool⁶² range from pure sheet (-1) to pure helix ($+1$). Secondary structure propensity for PGLa (A) in TFE/buffer (1 : 3 v/v) and (B) in aqueous buffer. The secondary structure propensities for pPGLc, pPGLa and PGLc in TFE/buffer (1 : 3 v/v) are depicted in (C, E and G), respectively, while the differences in structural propensity when compared with PGLa are shown in (D, F and H), respectively.

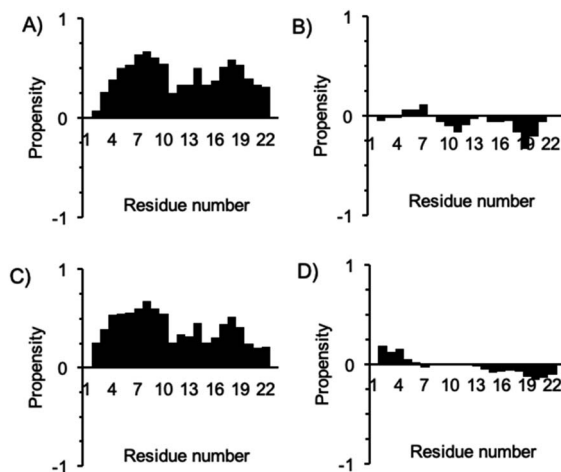


Fig. 2 Helix propensity of magainin 2 and the effect of terminal modifications. Secondary structure propensities determined using assigned chemical shifts and the ncSPC tool⁶² range from pure sheet (−1) to pure helix (+1). Secondary structural propensity for magainin 2a (A) in TFE/buffer (1 : 3 v/v) and (B) in aqueous buffer. The secondary structure propensity for pmagainin 2c in TFE/buffer (1 : 3 v/v) is depicted in (C), while the difference in structural propensity when compared with magainin 2c is shown in (D).

for both peptides (Fig. 1B and 2B), suggesting that the propensity of both peptides to form β -sheet amyloids⁶⁵ is already apparent under these conditions.

The TFE/buffer mixture serves as a simple membrane mimic with helix inducing properties.⁶⁶ All peptide variants showed a dominant helix structure in TFE/buffer (1 : 3 v/v), but variations were observed (Fig. 1 and 2). The N-terminus of PGLa is mostly unstructured, whereas residues 6 to 21 adopt a helical secondary structure in TFE/buffer (1 : 3 v/v) (Fig. 1A) in agreement with a gradual increase in structuration that has been observed early on in solid-state NMR investigations of bilayer-associated PGLa.⁶¹ When evaluating the structure of pPGLc, the N-terminus was mostly unaffected by the initial proline, whereas the carboxylic acid completely destroyed the helical structure at the C-terminus (Fig. 1C). Comparing the structural propensities of the two peptides reveals the degree of the structural changes (Fig. 1D). Evaluation of the secondary structure of pPGLa in TFE/buffer (1 : 3 v/v) confirmed that the proline induced only minor differences at the N-terminus and did not affect the structural propensity of the C-terminus (Fig. 1E and F).

Magainin 2a adopted a helical structure for most of the sequence, with a less structured segment around Lys11 and Phe12 (Fig. 2A). Introducing both the N-terminal proline and the free carboxy terminus did not induce major changes in the secondary structure (Fig. 2C and D). A slight increase in the helix propensity was observed for the N-terminus, whereas a slight decrease was observed for the C-terminus.

For all seven peptides the minimal inhibitory concentration preventing all growth (MIC_{100}) was determined as described earlier.⁵¹ The assay was performed at least twice for each peptide, with four replicas each time. Overall, the data is very consistent as shown by the averages and standard deviations depicted in

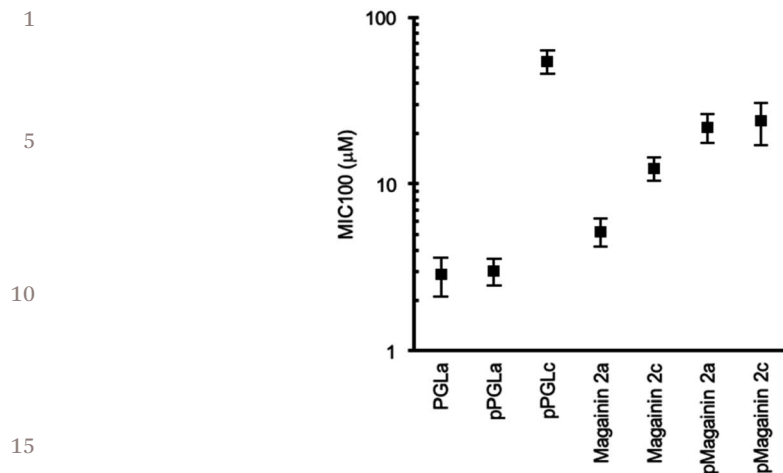


Fig. 3 Antibacterial activity of the magainin and PGLa variants investigated in this paper. The peptide concentration for 100% inhibition of *E. coli* bacterial growth (MIC₁₀₀) was determined for all peptide variants. The antimicrobial assays were repeated at least twice with four replicas each time. Error bars show the experimental standard deviations.

Fig. 3. For PGLa, we obtained a MIC₁₀₀ of $2.9 \pm 0.8 \mu\text{M}$ in excellent agreement with previously published values.⁵¹ The N-terminal proline did not affect the activity significantly, as we determined a MIC₁₀₀ of $3.0 \pm 0.6 \mu\text{M}$ for pPGLa (Fig. 3). On the other hand, the carboxy-terminus of pPGLc reduced the activity by a factor of 18 when compared to PGLa, as we determined a MIC₁₀₀ of $54 \pm 9 \mu\text{M}$. Within experimental error, pPGLc prepared by overexpression and by chemical synthesis has the same antibacterial activity (not shown).

For magainin, we found that a carboxy-terminus reduced the activity of magainin 2 by a factor of two as compared to magainin 2a, as the MIC₁₀₀ values were $5.2 \pm 1.0 \mu\text{M}$ and $12 \pm 2 \mu\text{M}$ for magainin 2a and magainin 2c, respectively (Fig. 3).⁵¹ The N-terminal proline had an even higher impact, as the activity of pmagainin 2a was reduced by a factor of four to $22 \pm 4 \mu\text{M}$. The combination of both an N-terminal proline and a carboxylic C-terminus did not result in any further reduction of the activity, as the MIC₁₀₀ of pmagainin 2c was $24 \pm 7 \mu\text{M}$.

By combining different variants of PGLa and magainin 2, we could evaluate the effects of the peptide termini on the PGLa–magainin synergism. All combinations of the two peptides resulted in increased activities compared to those expected for purely additive systems (Fig. 4A and B). Variation of the magainin 2 termini did not influence the synergism, as all mixtures of PGLa with any of the magainin 2 variants showed MIC₁₀₀ values of around $1 \mu\text{M}$ and synergy factors between four and five (Fig. 4A and C). Likewise, the N-terminal proline in pPGLa did not affect the synergistic activity of mixtures with variants of magainin 2 (Fig. 4, table). When combining pPGLc with magainin 2a, we obtained a similar enhancement of the activity as for PGLa–magainin 2a (Fig. 4D), but due to the significantly lower activity of pPGLc, the activity was slightly lower than that of the other mixtures with a MIC₁₀₀ value of $2.1 \pm 0.6 \mu\text{M}$ (Fig. 4B). The biggest enhancement of the antimicrobial activity, but also the lowest overall activity, was obtained when

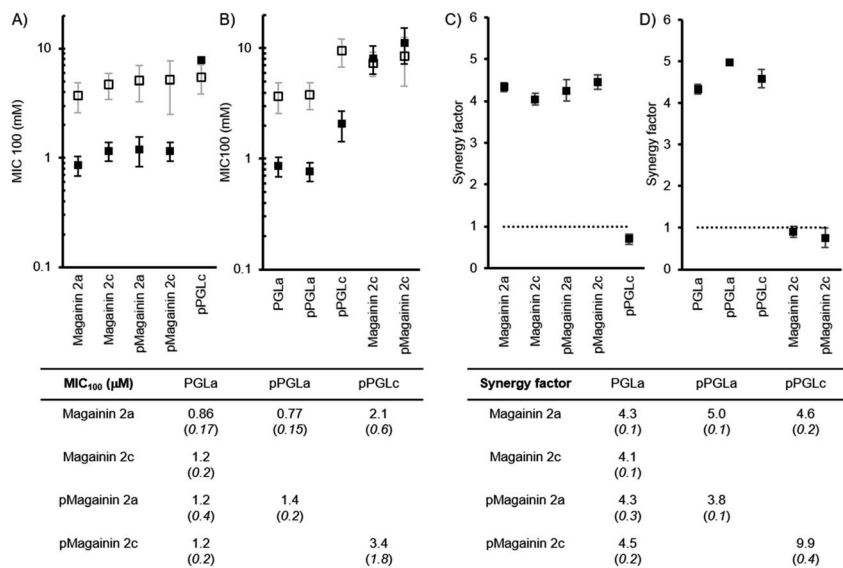


Fig. 4 Antibacterial activity of PGLa and magainin 2 mixtures. (A and B) experimental MIC₁₀₀ values for mixtures of PGLa and magainin 2a (black boxes), respectively, compared to the calculated MIC₁₀₀ values for 1 : 1 mixtures assuming the activities of the individual peptides are additive (open boxes). (C and D) calculated synergy factors for 1 : 1 mixtures containing PGLa and magainin 2a, respectively. The exact MIC₁₀₀ values (left) and calculated synergy factors (right) are listed in the tables together with the standard deviations in brackets. All experiments have been performed at least two times with four replicas each time. Error bars show either the experimental standard deviation or the calculated propagation of error.

pPGLc was mixed with pmagainin 2c. The MIC₁₀₀ was determined to be 3.4 ± 1.8 μM and the synergy factor was calculated to be 9.9 ± 0.4 (Fig. 4, tables).

As a control, we also combined two different variants of PGLa or two different variants of magainin 2. In these cases no change in activity when compared to the expected MIC₁₀₀ values was observed (Fig. 4A and B).

From the above-mentioned experiments, it is evident that the C-terminus plays a role in the antimicrobial activity of the individual peptides. However, the activity assays also revealed that the synergism between PGLa and magainin 2 is preserved for peptides with altered termini.

Discussion

The NMR structural characterization of peptides and proteins associated with lipid bilayers requires the introduction of isotope labels into the polypeptide sequence.⁵⁸ Bacterial overexpression remains an affordable and convenient method and offers the possibility to label the protein uniformly or selectively. To facilitate efficient bacterial expression and the purification of the resulting product, in many cases slight alterations are introduced into the native protein sequence. In the overexpression systems that we specifically designed to produce antimicrobial peptides in bacteria, tight inclusion bodies are formed due to the

1 presence of the TAF12 fusion protein.⁵⁹ Although this system provides proven
high yields of antimicrobial peptides in combination with a one-step purification,
the chemical cleavage of the TAF12 fusion tag using formic acid leaves an N-
terminal proline and the C-terminus is non-amidated. Because the peptide
5 termini clearly have a role in the overall activity of the peptides, the thus obtained
products were characterized here, thereby providing further insight into the
mechanism of synergistic interaction of these antimicrobial peptides.

Indeed, the antimicrobial activity of pPGLc is considerably decreased when
10 compared to PGLa (Fig. 3). This could be due to the additional negative charge at
the C-terminus or the decreased propensity of this sequence for helical structures
(Fig. 1). In the case of PGLa, the C-terminus appears to be more important than
the non-structured N-terminus,⁶¹ as the introduction of a proline prior to the
native sequence had no effect on the activity of the peptide (Fig. 3). On the other
15 hand, for magainin 2, the helix covers much of the sequence in membrane
mimetic environments^{60,67} and modifications of either terminus affect the activity
of the peptide (Fig. 3). Interestingly, we did not observe an additive effect for
alterations of both termini at the same time (Fig. 3).

Notably, membrane association of these peptides has been shown to be
20 strongly dependent on electrostatic interactions and these can be modulated by
changing the lipid composition^{40,42,64} or the peptide charge.⁶⁸ Therefore, the
reduced activity of the peptides carrying an additional negative charge at the C-
terminus is probably related to a reduction of attractive electrostatic interac-
tions at the bacterial surface.

25 Interestingly, the activity of the peptide mixtures pretty much follows the
activity of the PGLa variant (Fig. 4B) whereas the activity of the magainin 2 variant
has little influence (Fig. 4A). Indeed, it was concluded from recent calcein release
experiments that PGLa preconditions the insertion of magainin into membranes
with intrinsic negative curvature such as mixtures of POPE/POPG[†] (3/1 mole/
30 mole).⁴⁸ In a related manner, fluorescence correlation and fluorescence quen-
ching experiments show that fluorophore labelled PGLa helps magainin to associate
with POPE/POPG[†] membranes by formation of loosely interacting mesophases
made of the peptides.⁶⁹ Indeed, if such ‘helper activities’ of PGLa are reduced by
alterations of its termini, overall, fewer of the peptides interact with the
35 membrane and PGLa is expected to be the limiting factor determining the overall
activity of such mixtures (Fig. 4A and B).

Several structural models explaining the synergism between PGLa and mag-
ainin 2 have been proposed. Early on, cross-linking experiments with GGC-
40 extended PGLa and magainin sequences revealed the preferential formation of
parallel heterodimers in membranes.⁴⁷ Furthermore, in these early investigations
the negatively charged magainin E19 residue was found to be important. Based on
coarse grain MD simulations Vacha *et al.* found that salt bridges between this
magainin anionic charge and K12 and K15 of PGLa as well as hydrophobic
45 interactions are important.²⁹ Furthermore, the peptide dimers have been found to
align along the membrane surface where they further assemble into tetramers

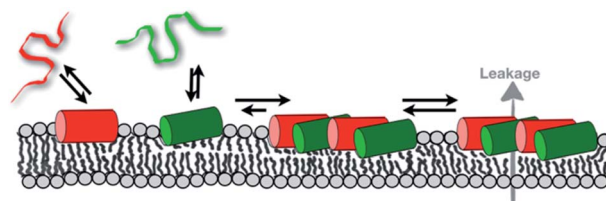
† Lipid abbreviations in this paper: CL: cardiolipin. DMPC: 1,2-dimyristoyl-*sn*-glycero-3-phosphocholine. DMPG: 1,2-dimyristoyl-*sn*-glycero-3-phospho-(1'-*rac*-glycerol). PC: phosphatidylcholine. PE: phosphatidylethanolamine. POPE: 1-palmitoyl-2-oleoyl-*sn*-glycero-3-phosphorylethanolamine. POPG: 1-palmitoyl-2-oleoyl-*sn*-glycero-3-phospho-(1'-*rac*-glycerol).

1 through C-terminal interactions.³³ At high concentrations, peptides of opposing
bilayers interact with each other, causing their adhesion. When sandwiched in
between lipid bilayers in this manner, the peptides cause membrane undulations
and accumulate in the resulting troughs where they form fibril-like assemblies.³³

5 Such C-terminal electrostatic interactions have also been found in previous
MD simulations of DMPC and DMPC/DMPG† membranes where the formation of
parallel heterodimers was driven by electrostatic interactions between the anionic
charges of magainin E19, its C-terminus and the lysines of PGLa at the 12, 15 and
10 19 positions.^{70–72} This heterodimerization was required for PGLa transmembrane
insertion which the authors correlated to the synergistic activities of the peptide
mixture.^{70,71} Thus, upon removal of the magainin negative charges, heterodimer
formation is disrupted and the bilayer insertion of PGLa is inhibited.⁷¹ In a follow-
up study, Zerweck *et al.* proposed a model of a large pore made of several
15 transmembrane PGLa homodimers, an arrangement which is held in place by C-
terminal interactions with in-plane oriented magainin 2.⁵⁷

Such an electrostatic interaction to stabilize heterodimers is unlikely when
both C-termini are negatively charged. The E19 residue, the carboxy terminus and
the helix dipole of magainin all add up to an overall electrical dipole on an
otherwise net cationic peptide (+3). Therefore, one would expect that removal of
20 a negative charge considerably weakens the electrostatic attraction to the even
more cationic PGLa helix (+5). As the synergistic effect was retained for the
pPGLc–pmagainin 2c mixture, the C-terminal interaction and its structural
implications are probably not crucial for the synergism even though they cause
25 a reduction of the antimicrobial activities of the individual peptides.

Furthermore, whereas the membrane topology of PGLa has been shown to be
dependent on the fatty acyl chain saturation,^{23,49} the synergistic formation of
pores is strongly correlated with the negative intrinsic curvature typically
observed with PE† head groups.^{48,69} Therefore, when models are established, it
30 seems wise to focus on biophysical data obtained with membranes closely
matching the composition of bacterial membranes.^{23,28,49,51} In membranes made
of *E. coli* lipid extracts, POPE/POPG or POPE/POPG/CL,† both peptides reside on
the membrane surface, therefore, realistic models of synergistic interactions
should be based on this topology.^{33,51,69} These models have in common that the
35 physico-chemical properties of the lipids, such as membrane intrinsic curva-
ture,⁴⁸ play an important role in the synergistic activity of the magainin/PGLa



40
45
50
Fig. 5 The equilibria that govern the membrane association and permeabilization of
membrane-associated magainin (red) and PGLa (green). The formation of mesophases,
which requires PE and negatively charged lipids, depletes the pool of monomers, thus
globally more peptide associates with the membrane. Furthermore, the high local peptide
density of the mesophase probably enhances membrane permeabilization.

1 mixture. Notably, mesophase arrangements of the peptides oriented along the
2 membrane surface have been detected in suitable membranes (Fig. 5) but not
3 when the PE lipid† was replaced by PC.^{51,69}

4 Importantly, the formation of such superstructures depletes the pool of
5 peptide monomers and increases the total amount of membrane-associated
6 peptides by an order of magnitude⁶⁹ which in itself can explain the increase in
7 antimicrobial and calcein release activities (Fig. 5). Furthermore, because the
8 synergistic action of PGLa and magainin requires the PE lipid,^{48,69} peptide
9 mixtures should not only be more active but also have an order of magnitude
10 higher therapeutic index when compared to the individual peptides.

11 The mesophase formation of peptides and lipids remains a puzzling obser-
12 vation and currently we can only speculate about the interactions that control
13 their assembly along the bilayer surface. Clearly, they are driven by the lipids
14 while at the same time the interactions retain specificity with regard to the
15 peptide sequences and the lipid composition. This is conceptually new and the
16 critical exchange among peers during the upcoming Faraday Discussion meeting
17 will be essential to advance such unconventional ideas. In this context, it is also
18 important that more experimental work is performed in the future to reveal the
19 structural details of such mesophases. Because the pPGLc and pmagainin 2c
20 constructs keep the high level of synergism (Fig. 4), it will be possible to use them
21 in their isotopically labelled forms for solid-state NMR investigations of the liquid
22 crystalline lipid bilayer.

23 Experimental

24 Solid-phase peptide synthesis

25 Three variants of PGLa (GMASK AGAIA GKI AK VALKA L-NH₂) and four variants of
26 magainin 2 (GIGKF LHS AK KFGKA FVGEI MNS-COOH) with different C-termini
27 and/or an additional N-terminal proline were prepared by solid-phase synthesis
28 using a Millipore 9050 automatic peptide synthesizer and Fmoc chemistry. The
29 peptides were purified by reverse phase HPLC (Gilson, Villiers-le-bel, France)
30 using a preparative C18 column (Luna, C-18-100 Å-5 µm, Phenomenex, Le Pecq,
31 France) and an acetonitrile/water gradient. Their identity and purity (>90%)
32 were checked by MALDI mass spectrometry (MALDI-TOF Autoflex, Bruker Daltonics,
33 Bremen, Germany). The purified peptides were dissolved three times in 2 mM HCl
34 at a 1 mg mL⁻¹ concentration with subsequent lyophilization to ensure exchange
35 of the TFA cations. Aliquots with 1 mg peptide were prepared and stored at
36 -20 °C.

37 Antimicrobial assays

38 For all activity assays, *E. coli* bacteria (ATCC25922, ref. 0335-CRM, Thermo Fisher
39 Scientific, Courtaboeuf, France) were grown overnight on Mueller-Hinton (MH)
40 agar plates. A suspension of bacteria in MH medium (Millipore, Sigma Aldrich,
41 Saint-Louis, MO, USA) was made from the plates and used to inoculate a 10 mL
42 preculture with a starting OD₅₅₀ = 0.005. The preculture was incubated overnight
43 and then used to inoculate a culture with a starting OD₅₅₀ = 0.2 (10 mL of MH).
44 The culture was incubated until an OD₅₅₀ = 1.0 was reached (after around 4
45 hours). From this culture, a standard bacterial suspension was prepared with
46

1 OD₅₅₀ = 0.2, which was used to prepare the final bacterial suspension at OD₅₅₀ = 0.0002.

5 The antimicrobial assays were performed in 96 well microplates (F-bottom sterile non-treated polystyrene, Thermo Scientific Nunc A/S, Roskilde, Denmark). All samples were added to the first column of the plate and subsequently exposed to a 1.5-fold dilution series in 21 steps. Finally, the bacterial suspension was distributed (50 μ L) to each well except the blank controls. The final peptide concentration ranged from 200 μ M to 0.04 μ M (after addition of bacteria).

10 The plates were incubated at 37 °C for 18 hours before the OD₆₀₀ was measured. Resazurin was added to each well (0.04 mg mL⁻¹ final concentration) and the plates were incubated for another two hours. The cell viability was determined based on the reduction of resazurin. The ratio of reduced resazurin was measured using the absorbance at 570 nm and 600 nm.

15

Data analysis

20 For each well, the ratio between the absorbance at 570 nm and the absorbance at 600 nm was calculated. The average value for the blank medium was then subtracted from all wells, before normalizing against the average values from wells containing bacteria but no peptide. The lowest peptide concentration where no reduction of resazurin was observed is considered the minimal inhibition concentration (MIC₁₀₀). Average values with standard deviations were calculated based on at least two experiments with four replicas each.

25 For 1 : 1 peptide mixtures, the expected MIC₁₀₀ value was calculated under the assumption of the peptide activities being additive (no synergism or antagonism) from eqn (1):

$$30 \quad \text{MIC}_{100}^{a+b} = 2 \frac{\text{MIC}_{100}^a \times \text{MIC}_{100}^b}{\text{MIC}_{100}^a + \text{MIC}_{100}^b} \quad (1)$$

with the two peptides denoted by *a* and *b*.

The synergy factor (1/CI) was calculated based on the observed MIC₁₀₀ of the mixtures from eqn (2):

$$35 \quad \text{CI} = \frac{0.5 \times \text{MIC}_{100}^{a+b}}{\text{MIC}_{100}^a} + \frac{0.5 \times \text{MIC}_{100}^{a+b}}{\text{MIC}_{100}^b} \quad (2)$$

with the two peptides denoted by *a* and *b* and their 1 : 1 mixture denoted by *a + b*.

40

Determination of helical propensity

45 The peptides were dissolved directly in 50 mM Tris (pH 7.4) or in a d₃-TFE/buffer (1 : 3 v/v) solution to give a final peptide concentration of 1 mg mL⁻¹. Trimethylsilylpropanoic acid (TSP) was added as an internal chemical shift reference. Two-dimensional ¹H-¹H TOCSY, ¹H-¹H NOESY and ¹H-¹³C HSQC spectra were acquired on a 500 MHz Bruker spectrometer equipped with a BBFO cryo probe (Bruker Biospin, Rheinstetten, Germany). Assignment was based on TOCSY and NOESY cross-peaks as well as typical amino acid chemical shifts.

50 The secondary structural propensity was calculated based on proton (H, HA, HB) and carbon (CA, CB) chemical shifts for all residues. The neighbour corrected Structural Propensity Calculator (ncSPC)⁶² online tool compensating for the

1 neighbour effects was used for the calculation, in order to obtain the most
accurate structural propensities: <https://st-protein02.chem.au.dk/ncSPC/>.

5 For the samples of PGLa and magainin 2a dissolved in aqueous buffer (50 mM
Tris, pH 7.4), the assignments were based on the random coil chemical shifts
calculated by the same online tool. As no correlations were observed in the NOESY
spectra and only small deviations from the random coil shifts were observed, we
consider the results to be reliable.


10 Conclusions

We tested the effect of adding a proline to the amino terminus of PGLa or mag-
ainin 2, as well as changing the chemical composition of their C-terminus. On
a structural level, some of these modifications changed the helix propensity and
the charge of the peptides. On a functional level, they have a strong effect on
15 antimicrobial activity, but retain the synergistic enhancement of the antimicro-
bial activity of the equimolar peptide mixtures. The latter observation makes
models of synergism where the two termini interact with each other unlikely.

20 Conflicts of interest

There are no conflicts to declare.

25 Acknowledgements

We gratefully acknowledge Delphine Hatey and Bruno Vincent for helping with
peptide synthesis and solution NMR spectroscopy, respectively. The discussions
with Martin Hof and Mariana Amaro are much appreciated. The financial
contributions of the Agence Nationale de la Recherche (projects MemPepSyn 14-
CE34-0001-01, Biosupramol 17-CE18-0033-3, Naturalarsenal 19-AMRB-0004-02
and the LabEx Chemistry of Complex Systems 10-LABX-0026_CSC), the Univer-
sity of Strasbourg, the CNRS, the Région Alsace and the RTRA International
30  Center of Frontier Research in Chemistry are gratefully acknowledged.

35 Notes and references

- 1 H. G. Boman, *Annu. Rev. Immunol.*, 1995, **13**, 61–92.
- 2 M. Zasloff, *Nature*, 2002, **415**, 389–395.
- 3 B. Agerberth, H. Gunne, J. Odeberg, P. Kogner, H. G. Boman and
G. H. Gudmundsson, *Proc. Natl. Acad. Sci. U. S. A.*, 1995, **92**, 195–199.
- 4 M. Pirtskhalava, A. Gabrielian, P. Cruz, H. L. Griggs, R. B. Squires, D. E. Hurt,
M. Grigolava, M. Chubinidze, G. Gogoladze, B. Vishnepolsky, V. Alekseyev,
45 A. Rosenthal and M. Tartakovsky, *Nucleic Acids Res.*, 2016, **44**, D1104–D1112.
- 5 G. Wang, X. Li and Z. Wang, *Nucleic Acids Res.*, 2016, **44**, D1087–D1093.
- 6 J. Cai, X. Li, H. Du, C. Jiang, S. Xu and Y. Cao, *Immunobiology*, 2020, 151936,
DOI: 10.1016/j.imbio.2020.151936.
- 7 E. Yuksel and A. Karakecili, *Mater. Sci. Eng., C*, 2014, **45**, 510–518.
- 8 D. Yang, R. Zou, Y. Zhu, B. Liu, D. Yao, J. Jiang, J. Wu and H. Tian, *Nanoscale*,
50 2014, **6**, 14772–14783.

- 1 9 K. Reijmar, K. Edwards, K. Andersson and V. Agmo Hernandez, *Langmuir*, 2016, **32**, 12091–12099.
- 10 D. Roversi, V. Luca, S. Aureli, Y. Park, M. L. Mangoni and L. Stella, *ACS Chem. Biol.*, 2014, **9**, 2003–2007.
- 5 11 L. A. Rollins-Smith, J. K. Doersam, J. E. Longcore, S. K. Taylor, J. C. Shamblin, C. Carey and M. A. Zasloff, *Dev. Comp. Immunol.*, 2002, **26**, 63–72.
- 12 D. P. Tieleman, B. Hess and M. S. Sansom, *Biophys. J.*, 2002, **83**, 2393–2407.
- 13 B. Bechinger, *J. Pept. Sci.*, 2015, **21**, 346–355.
- 10 14 C. Aisenbrey, A. Marquette and B. Bechinger, *Adv. Exp. Med. Biol.*, 2019, **1117**, 33–64.
- 15 C. J. Arnusch, H. B. Albada, M. van Vaardegem, R. M. J. Liskamp, H. G. Sahl, Y. Shadkchan, N. Osherov and Y. Shai, *J. Med. Chem.*, 2012, **55**, 1296–1302.
- 16 C. Ghosh, N. Harmouche, B. Bechinger and J. Haldar, *ACS Omega*, 2018, **3**, 9182–9190.
- 15 17 M. Laurencin, M. Simon, Y. Fleury, M. Baudy-Floc'h, A. Bondon and
■ B. Legrand, *Chem. – Eur. J.*, 2018, **24**, 6191–6201.
- 18 N. P. Chongsiriwatana, J. S. Lin, R. Kapoor, M. Wetzler, J. A. C. Rea, M. K. Didwania, C. H. Contag and A. E. Barron, *Sci. Rep.*, 2017, **7**, 16718.
- 20 19 L. A. Rank, N. M. Walsh, R. Liu, F. Y. Lim, J. W. Bok, M. Huang, N. P. Keller, S. H. Gellman and C. M. Hull, *Antimicrob. Agents Chemother.*, 2017, **61**, e00204–e00217.
- 20 H. G. Boman, *J. Intern. Med.*, 2003, **254**, 197–215.
- 25 21 K. Matsuzaki, O. Murase, H. Tokuda, S. Funakoshi, N. Fujii and K. Miyajima, *Biochemistry*, 1994, **33**, 3342–3349.
- 22 B. Bechinger, *J. Pept. Sci.*, 2011, **17**, 306–314.
- 23 E. Salnikov and B. Bechinger, *Biophys. J.*, 2011, **100**, 1473–1480.
- 24 E. Strandberg, D. Tiltak, S. Ehni, P. Wadhvani and A. S. Ulrich, *Biochim. Biophys. Acta*, 2012, **1818**, 1764–1776.
- 30 25 K. He, S. J. Ludtke, W. T. Heller and H. W. Huang, *Biophys. J.*, 1996, **71**, 2669–2679.
- 26 E. Salnikov, C. Aisenbrey, V. Vidovic and B. Bechinger, *Biochim. Biophys. Acta*, 2010, **1798**, 258–265.
- 35 27 C. Kim, J. Spano, E. K. Park and S. Wi, *Biochim. Biophys. Acta*, 2009, **1788**, 1482–1496.
- 28 N. Harmouche and B. Bechinger, *Biophys. J.*, 2018, **115**, 1033–1044.
- 29 M. Pachler, I. Kabelka, M. S. Appavou, K. Lohner, R. Vacha and G. Pabst, *Biophys. J.*, 2019, **117**, 1858–1869.
- 40 30 F. Y. Chen, M. T. Lee and H. W. Huang, *Biophys. J.*, 2003, **84**, 3751–3758.
- 31 A. Mecke, D. K. Lee, A. Ramamoorthy, B. G. Orr and M. M. Banaszak Holl, *Biophys. J.*, 2005, **89**, 4043–4050.
- 32 A. Farrotti, G. Bocchinfuso, A. Palleschi, N. Rosato, E. S. Salnikov, N. Voievoda, B. Bechinger and L. Stella, *Biochim. Biophys. Acta*, 2015, **1848**, 581–592.
- 45 33 I. Kabelka, M. Pachler, S. Prevost, I. Letofsky-Papst, K. Lohner, G. Pabst and R. Vacha, *Biophys. J.*, 2020, **118**, 612–623.
- 34 S. J. Ludtke, K. He, W. T. Heller, T. A. Harroun, L. Yang and H. W. Huang, *Biochemistry*, 1996, **35**, 13723–13728.
- 35 K. Matsuzaki, *Biochim. Biophys. Acta*, 1998, **1376**, 391–400.
- 50 36 Y. Shai, *Biochim. Biophys. Acta*, 1999, **1462**, 55–70.

- 1 37 H. Jenssen, P. Hamill and R. E. Hancock, *Clin. Microbiol. Rev.*, 2006, **19**, 491–511.
- 38 K. Hall, T. H. Lee, A. I. Mechler, M. J. Swann and M. I. Aguilar, *Sci. Rep.*, 2014, **4**, 5479.
- 5 39 J. M. Henderson, A. J. Waring, F. Separovic and K. Y. C. Lee, *Biophys. J.*, 2016, **111**, 2176–2189.
- 40 K. Matsuzaki, M. Harada, S. Funakoshi, N. Fujii and K. Miyajima, *Biochim. Biophys. Acta*, 1991, **1063**, 162–170.
- 10 41 T. Wieprecht, M. Beyermann and J. Seelig, *Biochemistry*, 1999, **38**, 10377–10378.
- 42 M. Wenk and J. Seelig, *Biochemistry*, 1998, **37**, 3909–3916.
- 43 C. Aisenbrey and B. Bechinger, *Langmuir*, 2014, **30**, 10374–10383.
- 44 M. Wenzel, A. I. Chiriac, A. Otto, D. Zweytick, C. May, C. Schumacher, R. Gust, H. B. Albada, M. Penkova, U. Kramer, R. Erdmann, N. Metzler-Nolte, 15 S. K. Straus, E. Bremer, D. Becher, H. Brotz-Oesterhelt, H. G. Sahl and J. E. Bandow, *Proc. Natl. Acad. Sci. U. S. A.*, 2014, **111**, E1409–E1418.
- 45 A. Vaz Gomes, A. de Waal, J. A. Berden and H. V. Westerhoff, *Biochemistry*, 1993, **32**, 5365–5372.
- 20 46 H. V. Westerhoff, M. Zasloff, J. L. Rosner, R. W. Hendler, A. de Waal, G. Vaz, P. M. Jongsma, A. Riethorst and D. Juretic, *Eur. J. Biochem.*, 1995, **228**, 257–264.
- 47 K. Matsuzaki, Y. Mitani, K. Akada, O. Murase, S. Yoneyama, M. Zasloff and K. Miyajima, *Biochemistry*, 1998, **37**, 15144–15153.
- 48 R. Leber, M. Pachler, I. Kabelka, I. Svoboda, D. Enkoller, R. Vácha, K. Lohner and G. Pabst, *Biophys. J.*, 2018, **114**, 1945–1954.
- 25 49 E. Strandberg, J. Zerweck, P. Wadhvani and A. S. Ulrich, *Biophys. J.*, 2013, **104**, L09–L11.
- 50 E. S. Salnikov, C. Aisenbrey, F. Aussenac, O. Ouari, H. Sarrouj, C. Reiter, P. Tordo, F. Engelke and B. Bechinger, *Sci. Rep.*, 2016, **6**, 20895.
- 30 51 E. Glattard, E. S. Salnikov, C. Aisenbrey and B. Bechinger, *Biophys. Chem.*, 2016, **210**, 35–44.
- 52 T. Hara, H. Kodama, M. Kondo, K. Wakamatsu, A. Takeda, T. Tachi and K. Matsuzaki, *Biopolymers*, 2001, **58**, 437–446.
- 53 S. L. Grage, S. Afonin, S. Kara, G. Buth and A. S. Ulrich, *Front. Cell Dev. Biol.*, 35 2016, **4**, 65.
- 54 J. Zerweck, E. Strandberg, J. Burck, J. Reichert, P. Wadhvani, O. Kukhareno and A. S. Ulrich, *Eur. Biophys. J.*, 2016, **45**, 535–547.
- 55 A. Marquette, E. Salnikov, E. Glattard, C. Aisenbrey and B. Bechinger, *Curr. Top. Med. Chem.*, 2015, **16**, 65–75.
- 40 56 B. Bechinger, *J. Mol. Biol.*, 1996, **263**, 768–775.
- 57 J. Zerweck, E. Strandberg, O. Kukhareno, J. Reichert, J. Burck, P. Wadhvani and A. S. Ulrich, *Sci. Rep.*, 2017, **7**, 13153.
- 58 R. Verardi, N. J. Traaseth, L. R. Masterson, V. V. Vostrikov and G. Veglia, *Adv. Exp. Med. Biol.*, 2012, **992**, 35–62.
- 45 59 US Pat., 61/065709, 2008.
- 60 B. Bechinger, M. Zasloff and S. J. Opella, *Protein Sci.*, 1993, **2**, 2077–2084.
- 61 B. Bechinger, M. Zasloff and S. J. Opella, *Biophys. J.*, 1998, **74**, 981–987.
- 62 K. Tamiola and F. A. Mulder, *Biochem. Soc. Trans.*, 2012, **40**, 1014–1020.
- 50 63 T. Wieprecht, O. Apostolov, M. Beyermann and J. Seelig, *J. Mol. Biol.*, 1999, **294**, 785–794.

- 1 64 T. Wieprecht, O. Apostolov, M. Beyermann and J. Seelig, *Biochemistry*, 2000, **39**,
442–452.
- 65 D. W. Juhl, E. Glattard, M. Lointier, P. Bampilis and B. Bechinger, 2020,
10 **9** submitted.
- 5 66 D. Marion, M. Zasloff and A. Bax, *FEBS Lett.*, 1988, **227**, 21–26.
- 67 J. Gesell, M. Zasloff and S. J. Opella, *J. Biomol. NMR*, 1997, **9**, 127–135.
- 68 K. Matsuzaki, A. Nakamura, O. Murase, K. Sugishita, N. Fujii and K. Miyajima,
Biochemistry, 1997, **36**, 2104–2111.
- 11** 69 C. Aisenbrey, M. Amaro, P. Pospisil, M. Hof and B. Bechinger, *Sci. Rep.*, 2020,
10 in press.
- 70 E. Strandberg, D. Horn, S. Reisser, J. Zerweck, P. Wadhvani and A. S. Ulrich,
Biophys. J., 2016, **111**, 2149–2161.
- 71 E. Han and H. Lee, *RSC Adv.*, 2015, **5**, 2047–2055.
- 15 72 A. Pino-Angeles, J. M. Leveritt III and T. Lazaridis, *PLoS Comput. Biol.*, 2016, **12**,
e1004570.
- 20
- 25
- 30
- 35
- 40
- 45
- 50